



MODELING OF THE HEAT TRANSFER IN A SUPERCRITICAL CO₂/DME MIXTURE FLOWING IN COOLED HELICALLY COILED TUBES

Yan Chen^a, Qingxin Ba^{b,*}, Xuefang Li^b

^a School of Energy and Power Engineering, Shandong University, Jinan 250061, China

^b Institute of Thermal Science and Technology, Shandong University, Jinan 250061, China

ABSTRACT

The heat transfer of supercritical CO₂/DME mixtures was modeled in this study for a mass ratio of 95/5 for cooling in horizontal helically coiled tubes. The CO₂/DME heat transfer coefficient was higher in the high-temperature zone than with pure CO₂. The heat transfer of CO₂/DME (95/5) was predicted for various mass fluxes, heat fluxes and pressures. The CO₂/DME heat transfer coefficient increased with the mass flux due to the increased turbulent diffusion, and first increased but then decreased with the heat flux. The peak heat transfer coefficient of CO₂/DME shifted toward the high-temperature region as the operating pressure increased. The effects of buoyancy and the centrifugal force were also analyzed to better understand the heat transfer mechanisms in helically coiled tubes. The gravitational buoyancy effect on the heat transfer decreased with mass flux while increased with heat flux. Higher heat fluxes strengthened the centrifugal buoyancy effect on the heat transfer at the beginning of the cooling process but weakened the centrifugal buoyancy effect later in the cooling process. The present study gives insight into the flow and heat transfer processes in helically coiled tubes which is useful for heat exchanger designs and refrigerant selection.

Keywords: CO₂/DME mixture, trans-critical system, heat transfer, heat pump

1. INTRODUCTION

The use of traditional chlorofluorocarbon (CFC), hydrochlorofluorocarbon (HCFC) and hydrofluorocarbon (HFC) refrigerants should be reduced because of global warming and ozone depletion (Groll, 2020). Natural working fluids such as ammonia (NH₃), hydrocarbons and carbon dioxide (CO₂) are attractive options for next generation refrigerants since they have zero ozone depletion potentials (ODP) and low global warming potentials (GWP). Among the natural working fluids, CO₂ is a promising refrigerant due to its favourable characteristics (non-toxic, non-flammable, high volumetric cooling capacity) and eco-friendly properties (ODP=0, GWP=1) so CO₂ has been used in heat pumps (Byrne *et al.*, 2009), air conditioners and other industrial processes (Kouta *et al.*, 2016; Milani *et al.*, 2017; Hou *et al.*, 2017; Leng *et al.*, 2016).

Due to the low critical temperature of CO₂ (31.1°C), CO₂ heat pumps use trans-critical cycles. Thus, the heat absorption occurs in the evaporator at subcritical conditions while the heat rejection takes place in the gas cooler at supercritical condition. The physical properties of supercritical fluids vary rapidly near the pseudo-critical point (Huang *et al.*, 2020). The heat transfer in supercritical CO₂ has been investigated for various temperatures, pressures, tube diameters, heat fluxes, mass fluxes and buoyancy forces. One of the most important heat transfer characteristics of supercritical CO₂ is the peak heat transfer coefficient near the pseudo-critical point which decreases with increasing pressure (Pitla *et al.*, 2001a; Pitla *et al.*, 2001b; Liao and Zhao, 2002a; Yoon *et al.*, 2003). The heat transfer rate increases with decreasing tube diameter for 1-7.75 mm tubes (Oh and Son, 2010; Dang and Hihara,

2004). The significant influence of buoyancy due to density variations causes the heat transfer to deteriorate for upward cooling flows, whereas the heat transfer rate increases for downward and horizontal flow during cooling (Jiang *et al.*, 2013; Li *et al.*, 2010; Wang *et al.*, 2017a). However, in trans-critical heat pumps, the gas cooler operating pressure exceeds the CO₂ critical pressure (7.38 MPa) and usually exceeds 10 MPa (Ehsan *et al.*, 2018), which requires high strength equipment and leads to large throttling losses (Kauf, 1999; Liao *et al.*, 2000; Austin and Sumathy, 2011).

Dimethyl ether (DME) also has outstanding thermophysical properties as a refrigerant such as high thermal conductivity, large latent heat, zero ODP and low GWP. However, pure DME cannot be directly used as a refrigerant due to its flammability (Liu *et al.*, 2018). However, mixtures of CO₂ and DME (CO₂/DME) use lower operating pressures than CO₂ trans-critical heat pumps while also suppressing the flammability of DME (Koyama *et al.*, 2006; Onaka *et al.*, 2008). The condensation (Afroz *et al.*, 2008) and evaporation (Onaka *et al.*, 2010) heat transfers of CO₂/DME mixtures flowing in horizontal smooth tubes have been experimentally studied for various mass fluxes. The results showed that the heat transfer coefficient increased with increasing DME mass fraction and that the pressure drops of CO₂/DME mixtures were lower than that of pure DME (Afroz *et al.*, 2008; Onaka *et al.*, 2010). However, as with pure CO₂, the heat rejection with CO₂/DME takes place at supercritical conditions. Previous studies of the heat transfer of CO₂/DME have been limited to condensation and evaporation processes for subcritical pressures. Therefore, more studies of the heat transfer characteristics of supercritical CO₂/DME are needed for designing gas coolers in heat pumps.

* Corresponding author. Email: qingxin90113@126.com

In addition, the secondary flow induced by the centrifugal force in helically coiled tubes leads to better heat transfer rates as seen in heat exchangers for various applications (Naphon and Wongwises, 2006; Gu *et al.*, 2020). Many studies have investigated the heat transfer in helically coiled tubes to study the effects of the geometric and flow parameters on the heat transfer (Ghorbani *et al.*, 2010; Piazza and Ciofalo, 2010; Chingulpitak and Wongwises, 2010; Ferng *et al.*, 2012). The supercritical CO₂ heat transfer coefficient in a helically coiled tube is higher than in a straight tube due to the coupled effects of the centrifugal and buoyancy forces (Zhang *et al.*, 2015; Yang, 2016; Xu *et al.*, 2016; Liu *et al.*, 2017).

In this study, the heat transfer was modeled for cooling of a supercritical CO₂/DME mixture in various horizontal helically coiled tubes. The heat transfer coefficients of a supercritical CO₂/DME mixture with a 5% DME mass fraction were calculated and compared with those of pure CO₂. Then, the heat transfer rates were calculated for various mass fluxes, heat fluxes and pressures. Finally, the effects of buoyancy and centrifugal forces were analyzed to provide a better understanding of the heat transfer mechanisms in a helically coiled tube.

2. NUMERICAL MODEL

2.1 Geometry and Grid

A three-dimensional geometry was created to model the horizontal helically coiled tube as shown in Fig. 1. The helical radius (R) was 18 mm, the tube radius (r) was 2 mm, the pitch (P) was 34 mm, and the total length of the helically coiled tube was 560 mm.

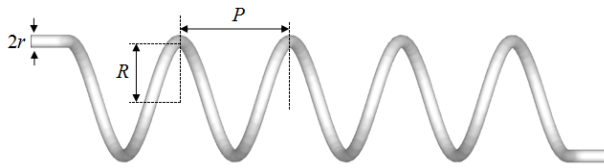


Fig. 1 Geometry

The computational domain was discretized into hexahedral elements using ANSYS ICEM as shown in Fig. 2. The wall y^+ was less than one to ensure the calculation accuracy near the wall. Four cases were calculated with four meshes of 315070, 447528, 630630 and 798720 cells for $p=8.0$ MPa, $T_{in}=320$ K, $G=239.2$ kg·m⁻²·s⁻¹ and $q=13.3$ kW·m⁻². The number of grid cells in the helically coiled tube section is described by a , b and c , as shown in Fig. 2, and the number of the elements along the tube is denoted by x . The detailed information of the four meshes is listed in Table 1. The calculated mean fluid temperatures are shown in Fig. 3. Similar results were obtained for Cases 3 and 4. The relative error in the fluid temperature was 0.002%. The calculations in this paper then used the mesh with 630630 elements.

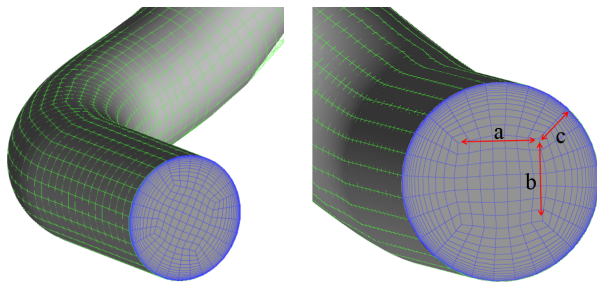


Fig. 2 Mesh in helically coiled tube

Table 1 Detailed information about four meshes

	a	b	c	x	Cells number
Case 1	5	5	11	1286	315070
Case 2	6	6	13	1286	447528
Case 3	7	7	14	1430	630630
Case 4	8	8	15	1560	798720

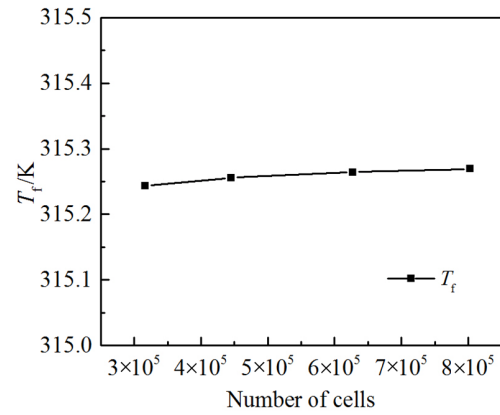


Fig. 3 Predicted fluid temperatures with four meshes

2.2 Numerical Model and Boundary Conditions

The flow and heat transfer processes follow the basic governing equations of fluid mechanics, including the continuity equation, momentum conservation equation and energy conservation equation. The continuity equation is

$$\frac{\partial \rho}{\partial t} + \nabla \cdot (\rho \vec{u}) = 0 \quad (1)$$

The momentum conservation equation is

$$\frac{\partial}{\partial t} (\rho \vec{u}) + \nabla \cdot (\rho \vec{u} \vec{u}) = -\nabla p + \nabla \cdot (\vec{\tau}) + \rho \vec{g} + \vec{F} \quad (2)$$

where p is the static pressure, $\vec{\tau}$ is the stress tensor, $\rho \vec{g}$ is the gravitational body force and \vec{F} is the external body forces. \vec{F} also contains other model-dependent source terms such as porous-media and user-defined sources.

The energy conservation equation is

$$\frac{\partial}{\partial t} (\rho T) + \nabla \cdot (\rho \vec{u} T) = \nabla \cdot \left(\frac{k}{c_p} \nabla T \right) + S_h \quad (3)$$

where S_h is the contribution of the viscous dissipation.

The Shear-Stress Transport (SST) $k-\omega$ model has been often used to accurately reproduce experimental data for heat transfer of supercritical CO₂ in helically coiled tubes in the literature (Wang *et al.*, 2015; Wang *et al.*, 2017b). The transport equations for the SST $k-\omega$ model are

$$\frac{\partial}{\partial t} (\rho k) + \frac{\partial}{\partial x_j} (\rho k u_j) = \frac{\partial}{\partial x_j} \left(\Gamma_k \frac{\partial k}{\partial x_j} \right) + G_k - Y_k \quad (4)$$

$$\frac{\partial}{\partial t} (\rho \omega) + \frac{\partial}{\partial x_j} (\rho \omega u_j) = \frac{\partial}{\partial x_j} \left(\Gamma_\omega \frac{\partial \omega}{\partial x_j} \right) + G_\omega - Y_\omega + D_\omega \quad (5)$$

where Γ is the effective diffusivity, G is the generation term, Y is the turbulent dissipation, and D represents the cross-diffusion term. The subscript k represents the turbulent kinetic and ω denotes the turbulent frequency.

The supercritical fluid was cooled in the horizontal helically coiled tube as shown in Fig. 4. The inlet boundary condition was a constant mass flux with a fixed pressure at the outlet. The wall boundary conditions were a no-slip boundary with a constant heat flux. The steady-state simulations were performed using Fluent which uses a

finite volume method to discretize the governing equations. The pressure-based solver was used. Velocity-pressure coupling used the Semi-Implicit Pressure-Linked Equation (SIMPLE) algorithm. The second-order upwind scheme was used to solve the turbulent kinetic energy equations and the QUICK scheme was used for the specific dissipation rate, momentum and energy equations. The thermophysical properties of CO₂ and CO₂/DME were derived from the NIST Standard Reference Database, including the specific heat, thermal conductivity, density and viscosity. Then, fitting formulae for the thermophysical properties of CO₂ and CO₂/DME were imported into the model through user defined functions.

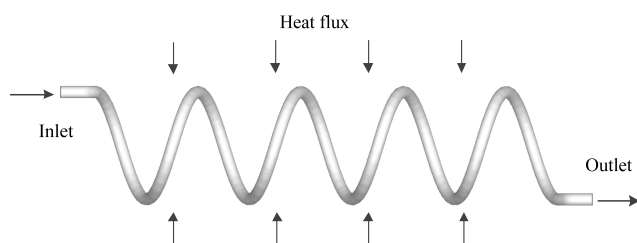


Fig. 4 Schematic of the computational model and boundary conditions

The calculations assumed that the tube wall was smooth and ignored the loss due to frictional resistance. The heat flux was assumed to be uniform and constant along the tube. The thermal effect of viscous dissipation was ignored.

The model was used to simulate CO₂/DME (95/5) cooling in the horizontal helically coiled tube for inlet temperatures of 300 to 345 K and pressures of 7.3 to 9.0 MPa. The heat fluxes ranged from 13.3 to 40 kW·m⁻² and the mass fluxes ranged from 239 to 430 kg·m⁻²·s⁻¹. The inlet *Re* varied from 1.33×10⁴ to 8.43×10⁴ as calculated by

$$Re = \frac{\rho u d}{\mu} \quad (6)$$

$$u = \frac{G}{\rho} \quad (7)$$

where *u* is the fluid velocity, *d* is the tube diameter, *G* is the mass flux, ρ is the density and μ is the dynamic viscosity.

The critical pressure of CO₂ is 7.38 MPa and the critical pressure of DME is 5.37 MPa. The critical pressure of the CO₂/DME (95/5) mixture is 7.28 MPa (Chen and Du, 2003)

$$P_{c,mixture} = \frac{23w_{CO_2} p_{c,CO_2} + 22w_{DME} p_{c,DME}}{23w_{CO_2} + 22w_{DME}} \quad (8)$$

where p_c is the critical pressure and *w* is the mass fraction.

2.3 Model Validation

Experimental results for supercritical CO₂ (Wang *et al.*, 2017b) were used to validate the numerical model. The experimental system included a low-temperature thermostat bath, a refrigerant pump, a mass flow meter, a pre-heater, a test section and a syringe pump, as shown in Fig. 5. In the test section, CO₂ flows inside the inner tube which is cooled by water in the annulus. The helically coiled copper tube was 560 mm long with an inner diameter of 4 mm and a coil pitch of 34 mm. The heat transfer coefficients were measured for various heat fluxes (9.0, 13.3 and 18.0 kW·m⁻²), mass fluxes (159.0, 239.2 and 318.2 kg·m⁻²·s⁻¹) and pressures (8.0, 8.5 and 9.0 MPa).

The experimental and calculated results for the average wall temperature and heat transfer coefficient are compared in Fig. 6. The inlet temperature ranged from 300 K to 330 K with a pressure of 8.0 MPa, mass flux of 239.2 kg·m⁻²·s⁻¹ and heat flux of 13.3 kW·m⁻², which

were consistent with the experimental conditions. As shown in Fig. 6, the predictions agree well with the experimental data.

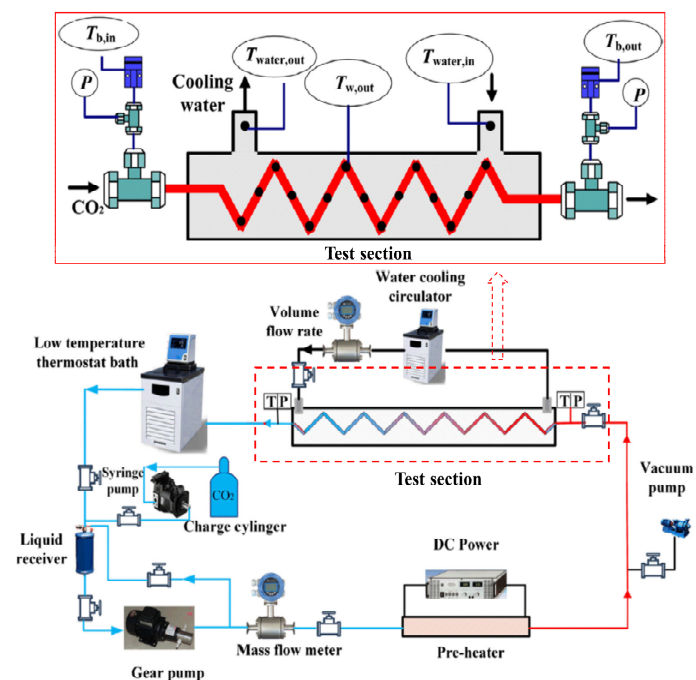
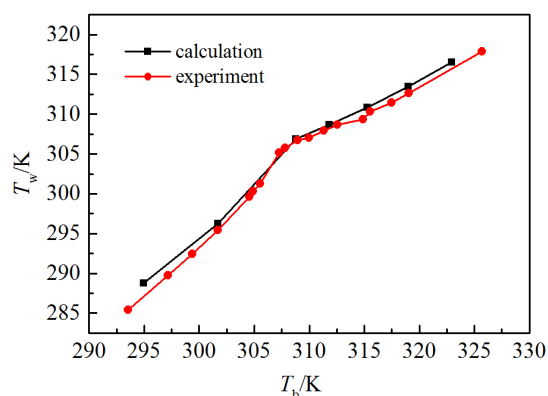
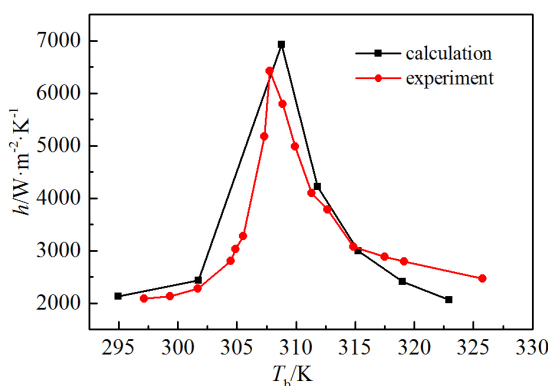


Fig. 5 Experimental system (Wang *et al.*, 2017b)



(a) Wall temperature



(b) Heat transfer coefficient

Fig. 6 Comparison of the predictions with experimental data (Wang *et al.*, 2017b)

3. RESULTS AND DISCUSSION

3.1 Comparison of the Heat Transfer between for Pure CO₂ and the CO₂/DME Mixture

The cooling of CO₂ and CO₂/DME (95/5) in horizontal helically coiled tubes was predicted for $p=8.0$ MPa, $q=13.3$ kW·m⁻², $G=239.2$ kg·m⁻²·s⁻¹ and $T_{in}=305$ -345 K. The heat transfer coefficients for the pure CO₂ and the CO₂/DME (95/5) mixture reached the peak values near their corresponding pseudo-critical temperatures as shown in Fig. 7. The peaks of the heat transfer coefficients are mainly due to the drastic changes in the thermophysical properties crossing the pseudo-critical point, especially the peak specific heat.

The CO₂/DME (95/5) peak heat transfer coefficient is less than that for pure CO₂ and is shifted to higher temperatures because of the smaller specific heat and larger pseudo-critical temperature in the mixture. The variation of the specific heat, regarded as the most influential thermophysical property for heat transfer [36], is shown in Fig. 8. The peak CO₂/DME (95/5) specific heat is less than that of pure CO₂. At the same time, the temperature where the specific heat reaches the maximum is higher for CO₂/DME (95/5), which indicates a higher pseudo-critical temperature. As shown in Fig. 7, the heat transfer coefficient of CO₂/DME is higher than that of pure CO₂ in the high-temperature region above 313 K. Therefore, CO₂/DME is more suitable for heat pumps with high heat rejection temperatures.

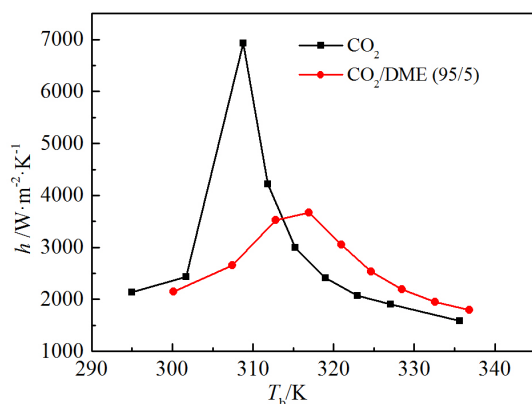


Fig. 7 CO₂ and CO₂/DME heat transfer coefficients

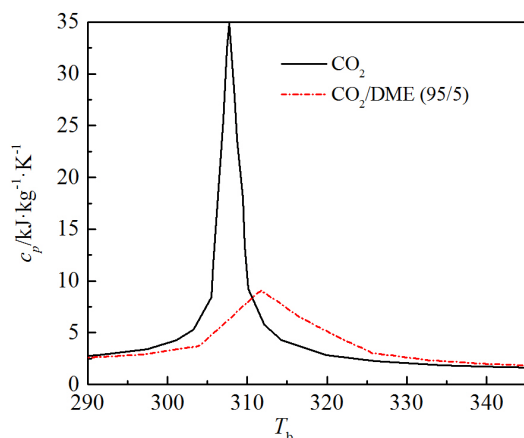
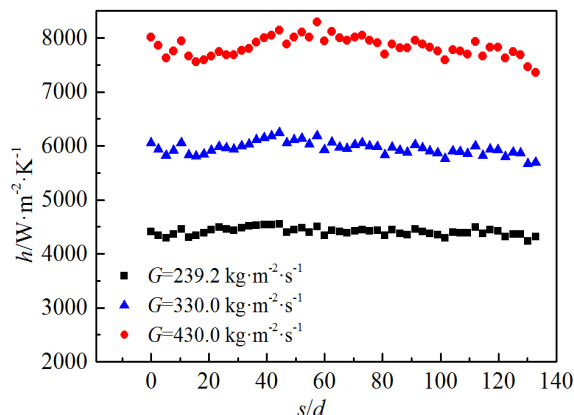


Fig. 8 CO₂ and CO₂/DME specific heat variations

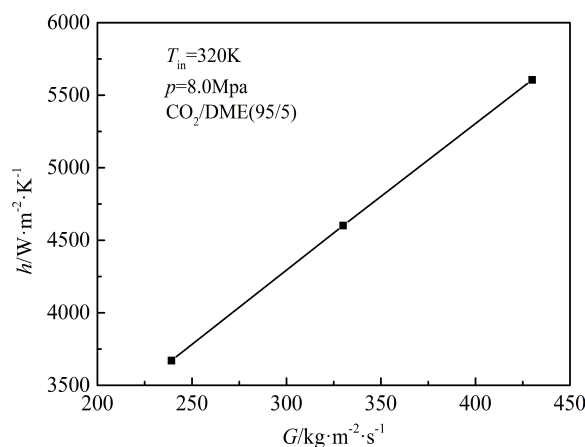
3.2 Effects of the Mass Flux, Heat Flux and Pressure

The effects of the mass flux on the heat transfer of the CO₂/DME mixture during cooling were modeled for CO₂/DME (95/5) at $p=8.0$

MPa, $q=13.3$ kW·m⁻², and $T_{in}=320$ K with mass fluxes of 239.2 to 430.0 kg·m⁻²·s⁻¹. The local heat transfer coefficients along the helically coiled tube and the mean heat transfer coefficients are shown in Fig. 9 for the various mass fluxes. The CO₂/DME heat transfer coefficient increases at higher mass fluxes due to the increased velocities and turbulent diffusion.



(a) Local heat transfer coefficients



(b) Mean heat transfer coefficients

Fig. 9 Mass flux effects on the CO₂/DME heat transfer coefficient

The effects of the heat flux on the heat transfer of CO₂/DME (95/5) is shown in Fig. 10. The heat flux varies from 13.3 to 40 kW·m⁻² at $p=8.0$ MPa, $G=239.2$ kg·m⁻²·s⁻¹ and $T_{in}=320$ K. The local heat transfer coefficients along the tube are shown in Fig. 10(a). As the cooling begins, the heat transfer coefficient increases with the heat flux. A possible explanation is that the density variation caused by the temperature difference increases with the heat flux and the increased buoyancy then enhances the heat transfer. As the cooling continues, the high heat flux rapidly cools the fluid to below the pseudo-critical temperature which reduces the heat transfer coefficient in Fig. 10(a). Therefore, near the outlet, the heat transfer coefficient is lowest at the highest heat flux. The mean heat transfer coefficients are shown in Fig. 10(b) for heat fluxes ranging from 13.3 to 40 kW·m⁻². The heat transfer coefficient initially increases with the heat flux because the fluid temperature is close to the pseudo-critical temperature. As the heat flux further increases at $q>25$ kW·m⁻², the bulk fluid temperature drops below the pseudo-critical temperature and the heat transfer coefficient decreases. The optimum heat flux is 25 kW·m⁻² in the present case at $p=8.0$ MPa, $G=239.2$ kg·m⁻²·s⁻¹ and $T_{in}=320$ K.

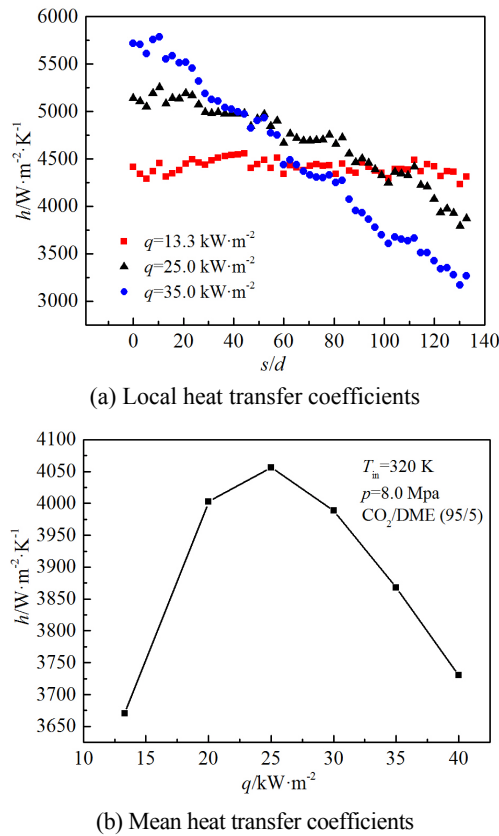


Fig. 10 Heat flux effects on the CO₂/DME heat transfer coefficient

The heat transfer coefficient of CO₂/DME (95/5) is shown in Fig. 11 as a function of the bulk temperature for various pressures for $G=239.2 \text{ kg}\cdot\text{m}^{-2}\cdot\text{s}^{-1}$ and $q=13.3 \text{ kW}\cdot\text{m}^{-2}$. In the low temperature region of 300-312 K, the heat transfer coefficient decreases as the pressure increases. The heat transfer coefficient then increases with pressure for $T>318 \text{ K}$. The heat transfer coefficients for the various pressures all increase gradually to a peak and then decrease with increasing fluid temperature. When the pressure increases, the peak heat transfer coefficient is nearly constant and shifts toward the high-temperature region. This is related to the pseudo-critical temperature of CO₂/DME (95/5) increasing with increasing pressure.

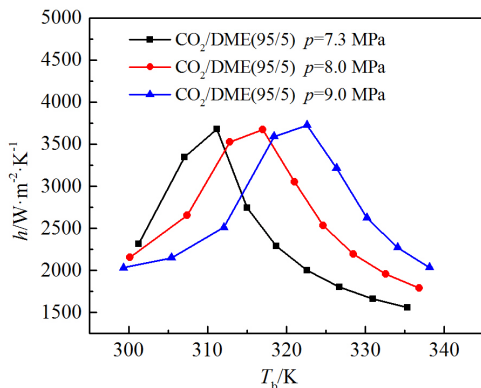


Fig. 11 Pressure effects on the CO₂/DME heat transfer coefficient

3.3 Effects of Buoyancy

The buoyancy effect due to the density variations is an important factor affecting the convective heat transfer in supercritical fluids. Flow in a helically coiled tube has both gravitational buoyancy and centrifugal buoyancy which are characterized by the gravitational Richardson number, Ri_g , and the centrifugal Richardson number, Ri_c , defined as (Yang, 2016; Xu *et al.*, 2016; Ciofalo *et al.*, 2015)

$$Ri_g = \frac{Gr_g}{Re^2} \quad (9)$$

$$Ri_c = \frac{Gr_c}{Re^2} \quad (10)$$

where the gravitational Grashof number, Gr_g , and the centrifugal Grashof number, Gr_c , are defined as

$$Gr_g = \frac{(\rho_w - \rho_f)\rho_f g d^3}{\mu_f^2} \quad (11)$$

$$Gr_c = \frac{\delta \rho_w - \rho_f}{4 \rho_f} Re^2 \quad (12)$$

The ratio of gravitational and centrifugal Richardson numbers characterizes the relative effects of the gravitational buoyancy force and the centrifugal buoyancy force as

$$\phi = Ri_g / Ri_c \quad (13)$$

3.3.1 Gravitational Buoyancy Force

The variation of gravitational Richardson number of CO₂/DME (95/5) with temperature is shown in Fig. 12 for $p=8.0 \text{ MPa}$, $G=239.2 \text{ kg}\cdot\text{m}^{-2}\cdot\text{s}^{-1}$, and $q=13.3 \text{ kW}\cdot\text{m}^{-2}$. Ri_g increases to a maximum near the pseudo-critical temperature and then drops as the bulk temperature increases further. Thus, the gravitational buoyancy effect is greatest around the pseudo-critical point.

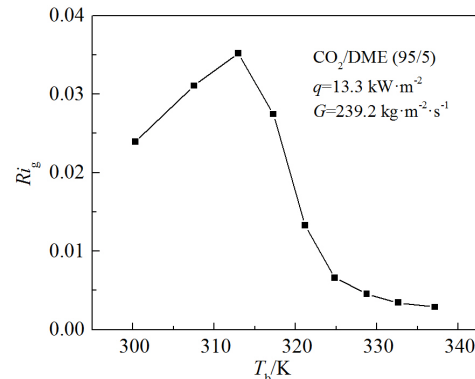


Fig. 12 Gravitational Richardson number for CO₂/DME at $p=8.0 \text{ MPa}$, $G=239.2 \text{ kg}\cdot\text{m}^{-2}\cdot\text{s}^{-1}$, and $q=13.3 \text{ kW}\cdot\text{m}^{-2}$.

The local gravitational Richardson numbers along the helically coiled tube are shown in Fig. 13 for various mass fluxes and heat fluxes at $p=8 \text{ MPa}$ and $T_{in}=320 \text{ K}$. The gravitational buoyancy decreases as the mass flux increases as shown in Fig. 13(a) and increases with the heat flux as shown in Fig. 13(b).

The effect of gravitational buoyancy on the heat transfer can be identified by comparing the cases with and without gravity. The heat transfer characteristics of supercritical CO₂/DME (95/5) without gravity were calculated for various mass fluxes and heat fluxes for $p=8 \text{ MPa}$ and $T_{in}=320 \text{ K}$. The local heat transfer coefficients are compared to those with gravity in Fig. 14. The heat transfer coefficients without gravity are lower than those with gravity, which indicates that the gravitational buoyancy force enhances the heat transfer for all cases. Previous studies have indicated that the gravitational buoyancy effect is negligible for $Ri_g<0.001$ (Liao and Zhao, 2002b). Others have suggested that the natural convection effect caused by gravitational buoyancy should be considered for $Ri_g>0.01$ (Yang, 2016; Xu *et al.*, 2016; Du *et al.*, 2010). In this study, the gravitational Richardson number Ri_g ranges from 0.024 to 0.007 for $G=430.0 \text{ kg}\cdot\text{m}^{-2}\cdot\text{s}^{-1}$ (Fig. 13), which is less than 0.01. Therefore, the threshold $Ri_g=0.01$ is

unreasonable for supercritical CO₂/DME because the gravitational buoyancy force significantly influences the heat transfer in all cases.

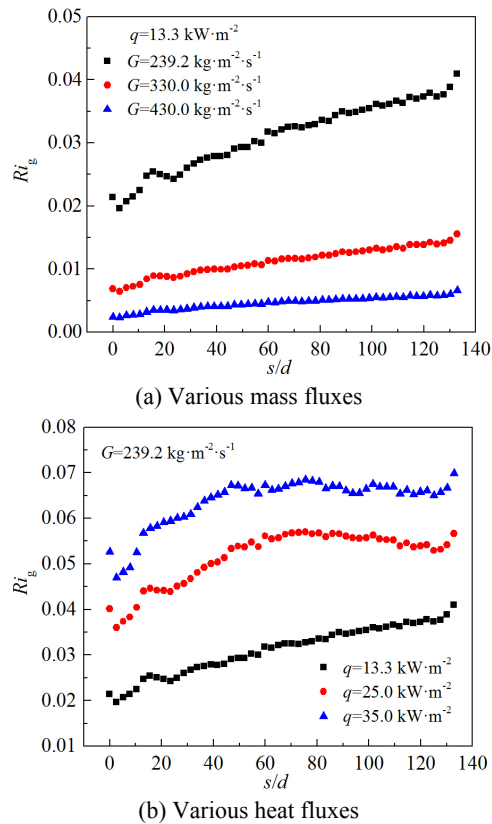


Fig. 13 Gravitational Richardson numbers for various mass fluxes and heat fluxes at $p=8$ MPa and $T_{in}=320$ K

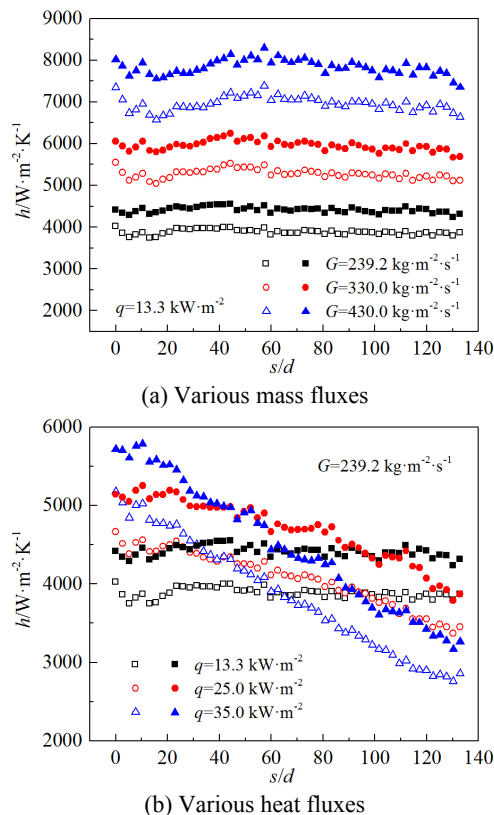


Fig. 14 Local heat transfer coefficients for $p=8$ MPa and $T_{in}=320$ K (Solid: with gravity; Hollow: without gravity)

3.3.2 Centrifugal buoyancy force

The centrifugal Richardson number is shown in Fig. 15 as a function of temperature for $p=8.0$ MPa, $G=239.2$ kg·m⁻²·s⁻¹ and $q=13.3$ kW·m⁻². As with the gravitational buoyancy effect, the centrifugal buoyancy effect also reaches a maximum around the pseudo-critical temperature. The variation of the Richardson number ratio with temperature is shown in Fig. 16. The Richardson number ratio, ϕ , decreases with increasing temperature from 14.2 to 0.93. Thus, the gravitational buoyancy has a large proportion in the liquid-like region at low temperatures, while the centrifugal buoyancy and the gravitational buoyancy both influence the heat transfer in the gas-like region at high temperatures.

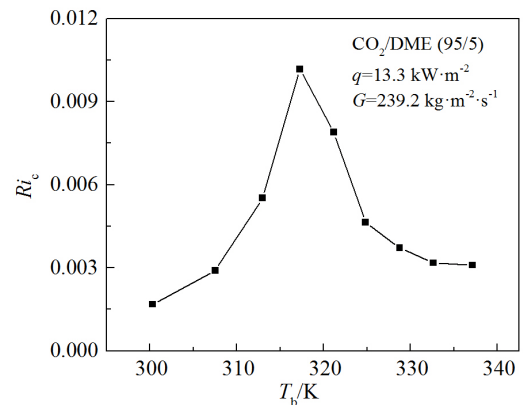


Fig. 15 Centrifugal Richardson numbers for CO₂/DME (95/5) at $p=8.0$ MPa

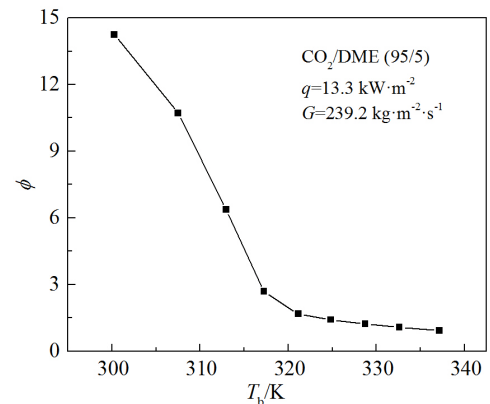


Fig. 16 Richardson number ratio for CO₂/DME (95/5)

The local centrifugal Richardson numbers along the helically coiled tube are shown in Fig. 17 for various mass fluxes and heat fluxes for $p=8.0$ MPa and $T_{in}=320$ K. The centrifugal buoyancy force decreases with mass flux due to the smaller density variations as shown in Fig. 17(a). The effect of the heat flux on the centrifugal buoyancy force is more complex as shown in Fig. 17(b). Ri_c initially increases with the heat flux and then tends to a constant. Near the tube outlet, Ri_c at $q=35$ kW·m⁻² becomes slightly lower than for the other cases. This can be explained by considering the definition of Ri_c in Eq. (7) and Eq. (9) and the density distributions in Fig. 18. At the beginning of the cooling, the higher heat flux results in larger density variations between the tube wall and the fluid, which strengthens the centrifugal buoyancy force. Later, the fluid is rapidly cooled by the heat fluxes, resulting in a significant increase in the fluid density. The density difference between the tube wall and the fluid decreases for $q=35$ kW·m⁻² since the density increase slows as the wall temperature cools from 312.6 K to 298 K as shown in Fig. 19. The rapid increase in the fluid density and the reduced density difference lead to the sharp decrease of Ri_c at $q=35$ kW·m⁻².

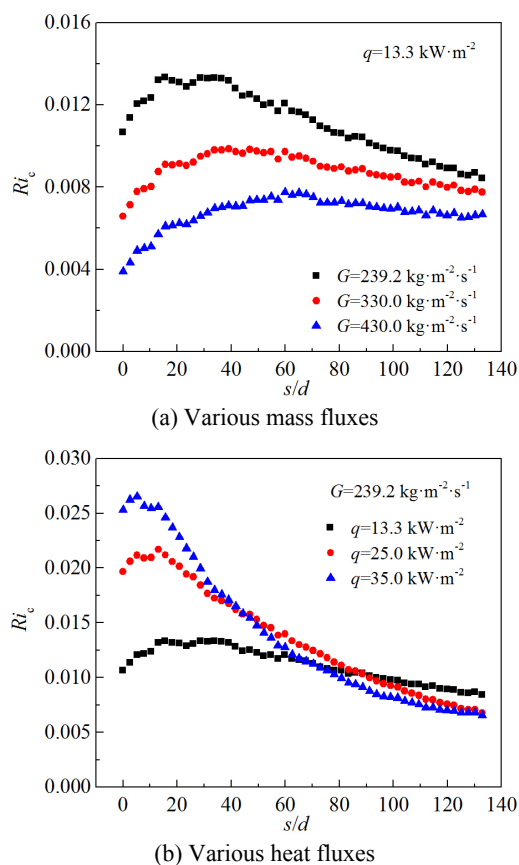


Fig. 17 Centrifugal Richardson numbers for various mass fluxes and heat fluxes for $p=8.0$ MPa and $T_{in}=320$ K.

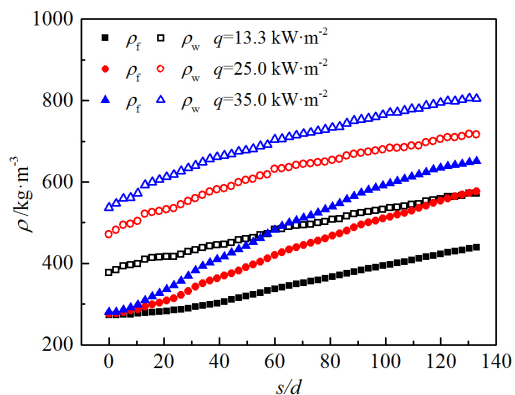


Fig. 18 Bulk and wall density variations for various heat fluxes

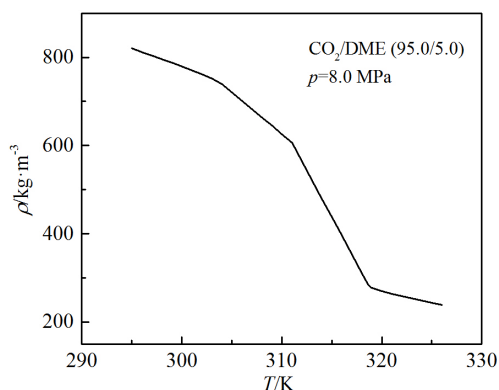


Fig. 19 CO₂/DME density as a function of temperature

The local gravitational and centrifugal Richardson number along the tube is plotted in Fig. 20 for various mass fluxes and heat fluxes for $p=8$ MPa and $T_{in}=320$ K. The Richardson number ratio decreases with increasing mass flux as shown in Fig. 20(a). The gravitational buoyancy plays a major role at the low mass flux ($G \leq 239.2$ kg·m⁻²·s⁻¹) while the centrifugal buoyancy plays a major role at the high mass flux ($G \geq 430.0$ kg·m⁻²·s⁻¹). Higher heat fluxes result in higher ϕ as shown in Fig. 20(b) which indicates that the effect of the gravitational buoyancy becomes increasing more important as the heat flux increases.

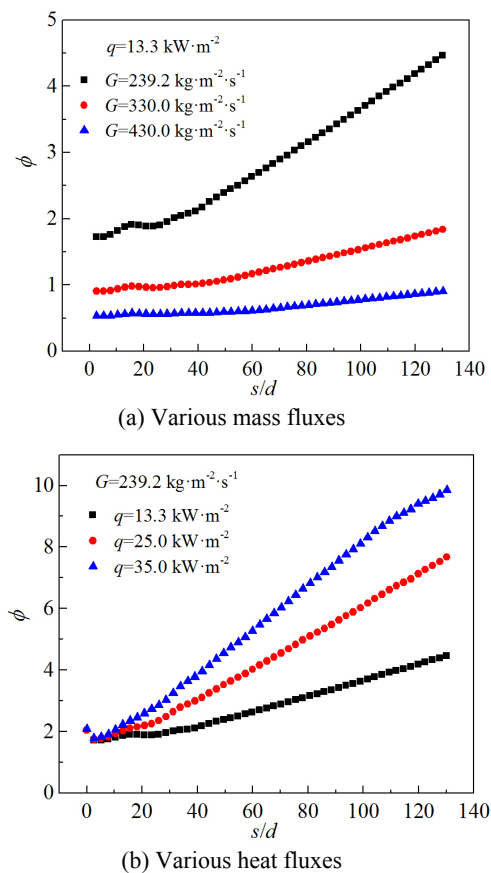


Fig. 20 Richardson number ratio for various mass fluxes and heat fluxes for $p=8$ MPa and $T_{in}=320$ K

4. CONCLUSIONS

The heat transfer characteristics of supercritical CO₂/DME during cooling were modeled for flow in a 4 mm inner diameter horizontal helically coiled tube. The CO₂/DME (95/5) heat transfer coefficients were compared with those for pure CO₂ flows. The results showed the effects of mass flux, heat flux and pressure on the heat transfer coefficients. The effects of the gravitational and centrifugal buoyancy forces were also analyzed to give a better understanding of the heat transfer mechanisms.

The CO₂/DME mixture was found to be more suitable than pure CO₂ for heat pumps with high heat rejection temperatures (above 313 K) due to the higher heat transfer coefficients. The peak heat transfer coefficient decreased and shifted to high temperatures for the CO₂/DME mixture. The peak heat transfer coefficient was 6931.5 kW·m⁻²·K⁻¹ at 309 K for the pure CO₂ and 3670.3 kW·m⁻²·K⁻¹ at 317 K for the CO₂/DME (95/5). The CO₂/DME heat transfer coefficient increased with the mass flux from 239.3 to 430.0 kg·m⁻²·s⁻¹ due to the increased turbulent diffusion. The heat transfer coefficient of CO₂/DME first increased but then decreased with the heat flux from 13.3 to 35.0 kW·m⁻². The optimum heat flux was 25 kW·m⁻² in the present study. The peak heat transfer coefficient of CO₂/DME shifted toward the high-

temperature region as the operating pressure increases, with temperature of 311 K for 7.3 MPa, 317 K for 8.0 MPa and 323 K for 9.0 MPa. The buoyancy effects caused by gravitational and centrifugal forces enhanced the heat transfer in horizontal helically coiled tubes. The gravitational buoyancy and centrifugal buoyancy effects reached their maximums near the pseudo-critical point. In the liquid-like region of CO₂/DME (300–317 K), the gravitational buoyancy more greatly influenced the heat transfer than the centrifugal buoyancy; while in the gas-like region (≥ 317 K), both the gravitational buoyancy and the centrifugal buoyancy influenced the heat transfer. The gravitational buoyancy increased with the mass flux but decreased with the heat flux. The centrifugal buoyancy decreased with the mass flux and initially increased with the heat flux while then tends to a constant.

This study provides further understanding of the heat transfer characteristics of supercritical CO₂/DME for refrigerant selection, operating parameters optimization and gas coolers design in trans-critical heat pumps.

NOMENCLATURE

c_p	specific heat ($J \cdot kg^{-1} \cdot K^{-1}$)
d	tube diameter (mm)
g	acceleration due to gravity ($m \cdot s^{-2}$)
G	mass flux ($kg \cdot m^{-2} \cdot s^{-1}$)
Gr	Grashof number
h	heat transfer coefficient ($W \cdot m^{-2} \cdot K^{-1}$)
k	turbulence kinetic energy ($J \cdot kg^{-1}$)
p	pressure (Pa)
P	coil pitch (mm)
Pr	Prandtl number
q	heat flux ($kW \cdot m^{-2}$)
r	tube radius (mm)
R	curvature radius (mm)
Re	Reynolds number
Ri	Richardson number
s	spiral length (mm)
T	temperature (K)
u	velocity ($m \cdot s^{-1}$)
x	mole fraction
y^+	non-dimensional distance from wall

Greek Symbols

δ	curvature ratio $\delta=r/R$
ρ	density ($kg \cdot m^{-3}$)
σ	turbulent Prandtl number
ω	specific dissipation rate (s^{-1})
ϕ	Richardson number ratio
μ	dynamic viscosity ($Pa \cdot s$)

Subscripts

pc	pseudo-critical
b	bulk
w	wall
f	fluid
g	gravity
c	centrifugal force

REFERENCES

Austin, B.T., and Sumathy, K., 2011, "Transcritical Carbon Dioxide Heat Pump Systems: A Review," *Renewable and Sustainable Energy Reviews*, **15**(8), 4013-4029.
<https://doi.org/10.1016/j.rser.2011.07.021>

Afroz, H.M.M., Miyara, A., and Tsubaki, K., 2008, "Heat Transfer Coefficients and Pressure Drops During In-tube Condensation of CO₂/DME Mixture Refrigerant," *International Journal of Refrigeration*, **31**(8), 1458-1466.
<https://doi.org/10.1016/j.ijrefrig.2008.02.009>

Byrne, P., Miriel, J., and Lenat, Y., 2009, "Design and Simulation of a Heat Pump for Simultaneous Heating and Cooling Using HFC or CO₂ as a Working Fluid," *International Journal of Refrigeration*, **32**(7), 1711-1723.
<https://doi.org/10.1016/j.ijrefrig.2009.05.008>

Chen, H.F., and Du, J.H., 2003, "Advanced Engineering Thermodynamics [M]," Beijing: Tsinghua University Press, 162-164.

Chingulpitak, S., and Wongwises, S., 2010, "Effects of Coil Diameter and Pitch on the Flow Characteristics of Alternative Refrigerants Flowing Through Adiabatic Helical Capillary Tubes," *International Communications in Heat and Mass Transfer*, **37**(9), 1305-1311.
<https://doi.org/10.1016/j.icheatmasstransfer.2010.07.005>

Ciofalo, M., Arini, A., and Liberto, M.D., 2015, "On the Influence of Gravitational and Centrifugal Buoyancy on Laminar Flow and Heat Transfer in Curved Pipes and Coils," *International Journal of Heat and Mass Transfer*, **82**, 123-134.
<https://doi.org/10.1016/j.ijheatmasstransfer.2014.10.074>

Dang, C., and Hihara, E., 2004, "In-tube Cooling Heat Transfer of Supercritical Carbon Dioxide. Part 1. Experimental Measurement," *International Journal of Refrigeration*, **27**(7):736-747.
<https://doi.org/10.1016/j.ijrefrig.2004.04.018>

Du, Z., Lin, W., and Gu, A., 2010, "Numerical Investigation of Cooling Heat Transfer to Supercritical CO₂ in a Horizontal Circular Tube," *The Journal of Supercritical Fluids*, **55**(1), 116-121.
<https://doi.org/10.1016/j.supflu.2010.05.023>

Ehsan, M.M., Guan, Z., and Klimenko, A.Y., 2018, "Comprehensive Review on Heat Transfer and Pressure Drop Characteristics and Correlations with Supercritical CO₂ under Heating and Cooling Applications," *Renewable and Sustainable Energy Reviews*, **92**, 658-675.
<https://doi.org/10.1016/j.rser.2018.04.106>

Ferng, Y.M., Lin, W.C., and Chieng, C.C., 2012, "Numerically Investigated Effects of Different Dean Number and Pitch Size on Flow and Heat Transfer Characteristics in a Helically Coil-tube Heat Exchanger," *Applied Thermal Engineering*, **36**, 378-385.
<https://doi.org/10.1016/j.applthermaleng.2011.10.052>

Ghorbani, N., Taherian, H., Gorji, M., and Mirgolbabaei, H., 2010, "Experimental Study of Mixed Convection Heat Transfer in Vertical Helically Coiled Tube Heat Exchangers," *Experimental Thermal and Fluid Science*, **34**(7), 900-905.
<https://doi.org/10.1016/j.expthermflusci.2010.02.004>

Hou, S., Wu, Y., Zhou, Y., and Yu, L., 2017, "Performance Analysis of the Combined Supercritical CO₂ Recompression and Regenerative Cycle Used in Waste Heat Recovery of Marine Gas Turbine," *Energy Conversion and Management*, **151**, 73-85.
<https://doi.org/10.1016/j.enconman.2017.08.082>

Huang, T., Li, X., and Cheng, L., 2020, "Modeling of the Flow and Heat Transfer of Supercritical CO₂ Flowing in Serpentine Tubes," *Frontiers in Heat and Mass Transfer*, **15**(15), 1-8.
<http://dx.doi.org/10.5098/hmt.15.15>

Jiang, P. X., Liu, B., Zhao, C.R., and Luo, F., 2013, "Convection Heat Transfer of Supercritical Pressure Carbon Dioxide in a Vertical Micro Tube from Transition to Turbulent Flow Regime," *International Journal of Heat and Mass Transfer*, **56**(1-2), 741-749.
<https://doi.org/10.1016/j.ijheatmasstransfer.2012.08.038>

Kauf, F., 1999, "Determination of the Optimum High Pressure for Transcritical CO₂-refrigeration Cycles," *International Journal of Thermal Sciences*, **38**(4), 325-330.
[https://doi.org/10.1016/S1290-0729\(99\)80098-2](https://doi.org/10.1016/S1290-0729(99)80098-2)

- Kouta, A., Al-Sulaiman, F., Atif, M., and Marshad, S.B., 2016, "Entropy, Exergy, and Cost Analyses of Solar Driven Cogeneration Systems Using Supercritical CO₂, Brayton Cycles and MEE-TVC Desalination System," *Energy Conversion and Management*, **115**, 253-264.
<https://doi.org/10.1016/j.enconman.2016.02.021>
- Koyama, S., Takato, N., Kuwahara, K., Jin, D., and Miyara, A., 2006, "Experimental Study on the Performance of a Refrigerant Mixture CO₂/DME System," In: *Proceedings of JSRAE Annual Conference*, Japan, 133-136.
- Leng, C., Wang, X.D., Yan, W.M., and Wang T.H., 2016, "Heat Transfer Enhancement of Microchannel Heat Sink Using Transcritical Carbon Dioxide as the Coolant," *Energy Conversion and Management*, **110**, 154-164.
<https://doi.org/10.1016/j.enconman.2015.12.006>
- Li, Z.H., Jiang, P.X., Zhao, C.R., and Zhang, Y., 2010, "Experimental Investigation of Convection Heat Transfer of CO₂ at Supercritical Pressures in a Vertical Circular Tube," *Journal of Supercritical Fluids*, **34**(8), 1162-1171.
<https://doi.org/10.1016/j.expthermflusci.2010.04.005>
- Liao, S.M., Zhao, T.S., and Jakobsen, A., 2000, "A Correlation of Optimal Heat Rejection Pressures in Transcritical Carbon Dioxide Cycles," *Applied Thermal Engineering*, **20**(9), 831-841.
[https://doi.org/10.1016/S1359-4311\(99\)00070-8](https://doi.org/10.1016/S1359-4311(99)00070-8)
- Liao, S.M., and Zhao, T.S., 2002a, "Measurements of Heat Transfer Coefficients from Supercritical Carbon Dioxide Flowing in Horizontal Mini/Micro Channels," *Journal of Heat Transfer*, **124**(3), 413-420.
- Liao, S.M., and Zhao, T.S., 2002b, "An Experimental Investigation of Convection Heat Transfer to Supercritical Carbon Dioxide in Miniature Tubes," *International Journal of Heat and Mass Transfer*, **45**(25), 5025-5034.
[https://doi.org/10.1016/S0017-9310\(02\)00206-5](https://doi.org/10.1016/S0017-9310(02)00206-5)
- Liu, X., Xu, X., Liu, C., Ye, J., Li, H., Bai, W., and Dang, C., 2017, "Numerical Study of the Effect of Buoyancy Force and Centrifugal Force on Heat Transfer Characteristics of Supercritical CO₂ in Helically Coiled Tube at Various Inclination Angles," *Applied Thermal Engineering*, **5**(7), 116-122.
<https://doi.org/10.1016/j.applthermaleng.2017.01.103>
- Liu, X., Xu, X., Liu, C., Bai, W., and Dang, C., 2018, "Heat Transfer Deterioration in Helically Coiled Heat Exchangers in Trans-critical CO₂ Rankine Cycles", *Energy*, **147**, 1-14.
<https://doi.org/10.1016/j.energy.2017.12.163>
- Groll, M., 2020, "Energy and Society: an Overview", *Frontiers in Heat and Mass Transfer*, **15**(2), 1-7.
<http://dx.doi.org/10.5098/hmt.15.2>
- Milani D, Luu M T, McNaughton R, and Abbas, A., 2017, "Optimizing an Advanced Hybrid of Solar-assisted Supercritical CO₂ Brayton Cycle: A Vital Transition for Low-Carbon Power Generation Industry," *Energy Conversion and Management*, **148**, 1317-1331.
<https://doi.org/10.1016/j.enconman.2017.06.017>
- Naphon, P., and Wongwises, S., 2006, "A Review of Flow and Heat Transfer Characteristics in Curved Tubes," *Renewable and Sustainable Energy Reviews*, **10**(5), 463-490.
<https://doi.org/10.1016/j.rser.2004.09.014>
- Oh, H.K., and Son, C.H., 2010, "New Correlation to Predict the Heat Transfer Coefficient In-tube Cooling of Supercritical CO₂ in Horizontal Macro-tubes," *Experimental Thermal and Fluid Science*, **34**(8):1230-1241.
<https://doi.org/10.1016/j.expthermflusci.2010.05.002>
- Onaka Y, Miyara A, Tsubaki K, and Koyama, S., 2008, "Analysis of Heat Pump Cycle Using CO₂/DME Mixture Refrigerant," *International Refrigeration and Air Conditioning Conference at Purdue*.
- Onaka, Y., Miyara, A., and Tsubaki, K., 2010, "Experimental Study on Evaporation Heat Transfer of CO₂/DME Mixture Refrigerant in a Horizontal Smooth Tube," *International Journal of Refrigeration*, **33**(7), 1277-1291.
<https://doi.org/10.1016/j.ijrefrig.2010.06.014>
- Piazza, I.D., and Ciofalo, M., 2010, "Numerical Prediction of Turbulent Flow and Heat Transfer in Helically Coiled Pipes," *International Journal of Thermal Sciences*, **49**(4), 653-663.
<https://doi.org/10.1016/j.ijthermalsci.2009.10.001>
- Pitla, S., Groll, E., and Ramadhyani, S., 2001a, "Convective Heat Transfer from In-tube Flow of Turbulent Supercritical Carbon Dioxide: Part 1—Numerical Analysis," *Hvac. and R. Research*, **7**(4), 345-366.
<https://doi.org/10.1080/10789669.2001.10391280>
- Pitla, S., Groll, E., and Ramadhyani, S., 2001b, "Convective Heat Transfer from In-tube Cooling of Turbulent Supercritical Carbon Dioxide: Part 2—Experimental Data and Numerical Predictions," *Hvac. and R. Research*, **7**(4), 367-382.
<https://doi.org/10.1080/10789669.2001.10391281>
- Wang, K., Xu, X., Wu, Y., Liu, C., and Dang, C., 2015, "Numerical Investigation on Heat Transfer of Supercritical CO₂ in Heated Helically Coiled Tubes," *Journal of Supercritical Fluids*, **99**, 112-120.
<https://doi.org/10.1016/j.supflu.2015.02.001>
- Wang, J., Guan, Z., Gurgenci, H., Hooman, K., Veeraragavan, A., and Kang, X., 2017a, "Computational Investigations of Heat Transfer to Supercritical CO₂ in a Large Horizontal Tube," *Energy Conversion and Management*, **157**, 536-548.
<https://doi.org/10.1016/j.enconman.2017.12.046>
- Wang, K., Xu, X., Liu, C., Bai, W., and Dang, C., 2017b, "Experimental and Numerical Investigation on Heat Transfer Characteristics of Supercritical CO₂ in the Cooled Helically Coiled Tube," *International Journal of Heat and Mass Transfer*, **108**, 1645-1655.
<https://doi.org/10.1016/j.ijheatmasstransfer.2017.01.004>
- Gu, X., Jiang, G., Wo, Y., and Chen, B., 2020, "Numerical Study on Heat Transfer Characteristics of Propylene Glycol-water Mixture in Shell Side of Spiral Wound Heat Exchanger", *Frontiers in Heat and Mass Transfer*, **15**(3), 1-8.
<http://dx.doi.org/10.5098/hmt.15.3>
- Xu, X.X., Liu, C., Dang, C., Wu, Y., and Liu, X., 2016, "Experimental Investigation on Heat Transfer Characteristics of Supercritical CO₂ Cooled in Horizontal Helically Coiled Tube," *International Journal of Refrigeration*, **67**, 190-201.
<https://doi.org/10.1016/j.ijrefrig.2016.03.010>
- Yang, M., 2016, "Numerical Study of the Heat Transfer to Carbon Dioxide in Horizontal Helically Coiled Tubes under Supercritical Pressure," *Applied Thermal Engineering*, **109**, 685-696.
<https://doi.org/10.1016/j.applthermaleng.2016.08.121>
- Yoon, S.H., Kim, J.H., Hwang, Y.W., Kim, M.S., Min, K., and Kim, Y., 2003, "Heat Transfer and Pressure Drop Characteristics during the In-tube Cooling Process of Carbon Dioxide in the Supercritical Region," *International Journal of Refrigeration*, **26**(8), 857-864.
[https://doi.org/10.1016/S0140-7007\(03\)00096-3](https://doi.org/10.1016/S0140-7007(03)00096-3)
- Zhang, W., Wang, S., Li, C., and Xu, J., 2015, "Mixed Convective Heat Transfer of CO₂ at Supercritical Pressures Flowing upward through a Vertical Helically Coiled Tube," *Applied Thermal Engineering*, **88**, 61-70.
<https://doi.org/10.1016/j.applthermaleng.2014.10.031>